1-1-2022

# Regulation of rod photoreceptor function by farnesylated G-protein γ-subunits

Alexander V. Kolesnikov

Elena Lobysheva

Jaya P. Gnana-Prakasam

Vladimir J. Kefalov

Oleg G. Kisselev

PLOS ONE

RESEARCH ARTICLE

# Regulation of rod photoreceptor function by farnesylated G-protein γ-subunits

**Alexander V. Kolesnikov[1,2], Elena Lobysheva[3], Jaya P. Gnana-Prakasam[3,4], Vladimir J. Kefalov[1,2,5]*, Oleg G. Kisselev[3,4]***

**1** Department of Ophthalmology, Gavin Herbert Eye Institute, University of California, Irvine, CA, United States of America, **2** Department of Ophthalmology and Visual Sciences, Washington University School of Medicine, St. Louis, Missouri, United States of America, **3** Department of Ophthalmology, Saint Louis University School of Medicine, Saint Louis, Missouri, United States of America, **4** Department of Biochemistry and Molecular Biology, Saint Louis University School of Medicine, Saint Louis, Missouri, United States of America, **5** Department of Physiology and Biophysics, University of California, Irvine, CA, United States of America

* kisselev@slu.edu (OGK); vkefalov@uci.edu (VJK)





**Citation:** Kolesnikov AV, Lobysheva E, Gnana-Prakasam JP, Kefalov VJ, Kisselev OG (2022) Regulation of rod photoreceptor function by farnesylated G-protein γ-subunits. PLoS ONE 17(8): e0272506. https://doi.org/10.1371/journal.pone.0272506

**Editor:** Steven Barnes, Doheny Eye Institute/UCLA, UNITED STATES

**Received:** April 7, 2022

**Accepted:** July 20, 2022

**Published:** August 8, 2022



**Data Availability Statement:** All relevant data are within the paper and its Supporting Information files.

**Funding:** This work was supported by National Institute of Health (https://www.nih.gov) grants EY018107 and EY028914 (O.G.K.), EY031008 (J.P.G.), EY025696 and EY030912 (V.J.K.) and unrestricted grants from Research to Prevent Blindness (https://www.rpbusa.org) to the Department of Ophthalmology and Visual Sciences at Washington University in St. Louis and the

## Abstract

Heterotrimeric G-protein transducin, Gt, is a key signal transducer and amplifier in retinal rod and cone photoreceptor cells. Despite similar subunit composition, close amino acid identity, and identical posttranslational farnesylation of their Gγ subunits, rods and cones rely on unique $G\gamma_1$ (*Gngt1*) and $G\gamma_c$ (*Gngt2*) isoforms, respectively. The only other farnesylated G-protein γ-subunit, $G\gamma_{11}$ (*Gng11*), is expressed in multiple tissues but not retina. To determine whether $G\gamma_1$ regulates uniquely rod phototransduction, we generated transgenic rods expressing $G\gamma_1$, $G\gamma_c$, or $G\gamma_{11}$ in $G\gamma_1$-deficient mice and analyzed their properties. Immunohistochemistry and Western blotting demonstrated the robust expression of each transgenic Gγ in rod cells and restoration of $G\alpha_{t1}$ expression, which is greatly reduced in $G\gamma_1$-deficient rods. Electroretinography showed restoration of visual function in all three transgenic $G\gamma_1$-deficient lines. Recordings from individual transgenic rods showed that photosensitivity impaired in $G\gamma_1$-deficient rods was also fully restored. In all dark-adapted transgenic lines, $G\alpha_{t1}$ was targeted to the outer segments, reversing its diffuse localization found in $G\gamma_1$-deficient rods. Bright illumination triggered $G\alpha_{t1}$ translocation from the rod outer to inner segments in all three transgenic strains. However, $G\alpha_{t1}$ translocation in $G\gamma_{11}$ transgenic mice occurred at significantly dimmer background light. Consistent with this, transretinal ERG recordings revealed gradual response recovery in moderate background illumination in $G\gamma_{11}$ transgenic mice but not in $G\gamma_1$ controls. Thus, while farnesylated Gγ subunits are functionally active and largely interchangeable in supporting rod phototransduction, replacement of retina-specific Gγ isoforms by the ubiquitous $G\gamma_{11}$ affects the ability of rods to adapt to background light.

## Introduction

The high sensitivity of rod photoreceptors is achieved by the activation of multiple copies of the heterotrimeric G-protein, Gt, by a single rhodopsin [1]. The Gtβγ ($G\beta_1\gamma_1$) complex is

Department of Ophthalmology at the University of California Irvine. The funders had no role in study design, data collection and analysis, decision to publish, or preparation of the manuscript.

**Competing interests:** The authors have declared that no competing interests exist.


**Fig 1. Multiple amino acid sequence alignment of mouse rod $G\gamma_1$ (*Gngt1*), cone $G\gamma_c$ (*Gngt2*), and $G\gamma_{11}$ (*Gng11*).**

https://doi.org/10.1371/journal.pone.0272506.g001

crucial for efficient signal amplification in mouse rods. Analysis of $G\gamma_1$-deficient rods has shown that although $G\alpha_{t1}$ is sufficient for signal transduction, the efficient signal amplification required for nocturnal vision is achieved only in the presence of the Gtβγ-complex [2, 3]. Whether the isoform diversity among Gγ-subunits contributes to specific physiological characteristics of retinal photoreceptors remains unknown. For example, rod and cone Gt heterotrimers are considered unique and the sole signal transducers in rods and cones respectively, compared to other cell types that contain multiple G-protein isoforms. Replacing individual subunits in retinal photoreceptors is a powerful approach to address their functional differences. Each of the three subunits of transducin, rod $G\alpha_{t1}$ vs. cone $G\alpha_{t2}$, rod $G\beta_1$ vs. cone $G\beta_3$, and rod $G\gamma_1$ vs. cone $G\gamma_c$, can potentially contribute to the observed lower rate of Gt activation in cones. With rare exception [4], the majority of the data obtained from $G\alpha_{t1}$ replacement experiments point to close functional similarity and good interchangeability between $G\alpha_{t1}$ and $G\alpha_{t2}$ [5–7]. Thus, the lower visual sensitivity of cones compared to rods and reduced rate of signal transduction between the cone visual pigment and PDE cannot be explained by the differences in the Gtα subunits.

G-protein γ-subunits are a protein family composed of twelve isoforms that are posttranslationally isoprenylated and carboxymethylated [8–11]. Only three Gγ subunits are modified by a 15-carbon farnesyl, while the rest contain a 20-carbon geranylgeranyl lipid moiety. The three farnesylated Gγ subunits are: rod-specific $Gt\gamma_1$ ($G\gamma_1$, *Gngt1*) [12]; cone-specific $Gt\gamma_c$ ($G\gamma_c$, $G\gamma_9$, *Gngt2*) [13]; and the relatively ubiquitous $G\gamma_{11}$ (*Gng11*) [14]. Rod and cone subunits of transducin share fairly high levels of amino acid identity: $G\alpha_{t1}$ is 78% identical to $G\alpha_{t2}$, $G\beta_1$ is 80% identical to $G\beta_3$, while $G\gamma_1$ is 64% identical to $G\gamma_c$ (Fig 1). Despite their similarities, Gγ subunits differ dramatically in their tissue expression pattern and putative G-protein coupled receptor (GPCR) partners [15, 16]. The reason for this intriguing diversity of Gγ subunits and the contribution of their amino acid sequence and protein structure in G-protein signaling remain very poorly understood. Thus, it is still a mystery why $G\gamma_1$ is specifically expressed in the rod photoreceptors and $G\gamma_c$ is exclusive to the cones, while $G\gamma_{11}$ is excluded from both photoreceptor types.

The determination of physiological roles of Gγ subunits in non-photoreceptor cells is difficult due to the redundancy of G-protein mediated pathways [17]. Phototransduction in rods, however, is mediated by a single G-protein transducin, Gtαβγ ($G\alpha_{t1}$, $G\beta_1$, $G\gamma_1$). Deletion of *Gngt1* to generate $G\gamma_1$-deficient mice results in rods with greatly reduced signal amplification and is associated with severe reduction in the expression of $G\alpha_{t1}$ and $G\beta_1$ [2]. To address how the specific properties of Gγ regulate the function of rods, we created transgenic mice expressing the rod $G\gamma_1$, the cone $G\gamma_c$, or the ubiquitous $G\gamma_{11}$ in the *Gngt1*$^{-/-}$ line. This approach allowed us to determine whether substitution of $G\gamma_1$ by $G\gamma_c$ or $G\gamma_{11}$ restores rod function. We also analyzed how the expression of each Gγ affects the expression of $G\alpha_{t1}$ and $G\beta_1$, as well as their light-driven translocation within rods.

## Materials and methods

### Generation of Gγ transgenic mouse lines

All experiments were performed in accordance with the Guide for the Care and Use of Laboratory Animals and were approved by the Saint Louis University Institutional Animal Care and

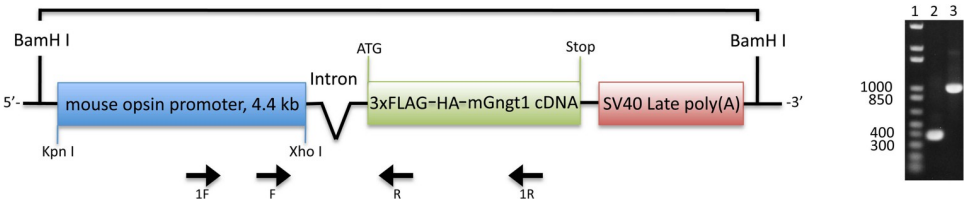


**Fig 2.** $G\gamma_1$ transgenic construct (left) and the PCR screening test (right). DNA gel: 1) Molecular weight markers; 2) 349 bp PCR product using universal F/R primers; 3) 1011 bp PCR product using 1F/1R primers. Similar design was employed to generate $G\gamma_c$ and $G\gamma_{11}$ transgenic constructs.

https://doi.org/10.1371/journal.pone.0272506.g002

Use Committee and the Washington University Animal Studies Committee. Unless otherwise specified, all mice were age-matched 2- to 3-month-old littermates of either sex; they were kept under the standard 12 h dark/light cycle and dark-adapted overnight before all experiments.

We introduced three individual mouse Gγ-subunits into $G\gamma_1$-deficient rods [18]. All transgenic constructs included the 4.4 kb mouse opsin promoter (generous gift from Dr. Lem, Tufts Medical Center) [19], mouse Gngt1 cDNA, as well as appropriate intron and poly(A) sequences (Fig 2). An in-frame insertion of 3xFLAG-HA epitope at the N-terminus of all Gγ was designed to help with detection and quantification of the expressed proteins. The following nucleic acid sequence was present in all individual synthetic genes used to generate the three transgenic constructs: `tttaaactgcagaagttggtcgtgaggcactgggcaggtaagtatcaaggttacaagacaggtttaaggagaccaatagaaactgggcttgtcgagacagagaagactcttgcgtttctgataggcacctattggtcttactgacatccactttgcctttctctccacaggtgtccactcccagttcaattacagctcttaaggctagagtacttaatacgactcactataggctagcctcgatcgagaattcacgcgtcttccctgacagaagatggactacaaagaccatgacggtgattataaagatcatgacatcgattacaaggatgacgatgacaagcttgcggccgcgaattcatacccatacgacgtaccagattacgct`.

It included part of the intron and 3xFLAG-HA epitope, and was used for developing genotyping assay at Transnetyx, Inc. The genotyping strategy is available for sharing upon request. The purified *BamH1* insertion fragment was microinjected into fertilized mouse eggs and re-implanted in pseudopregnant C57Bl/6 female mice. Founders expressing $G\gamma_1$, $G\gamma_c$, and $G\gamma_{11}$ transgenes were bred with our existing $G\gamma_1$-deficient line, *Gngt1*$^{-/-}$, to generate $G\gamma_1{}^{+}Gngt1^{-/-}$, $G\gamma_c{}^{+}Gngt1^{-/-}$, and $G\gamma_{11}{}^{+}Gngt1^{-/-}$ mice.

## Western blotting and antibodies

Retinas from 2-month-old dark-adapted mice were dissected, flash-frozen in liquid nitrogen, and stored at -80˚C until protein quantification or biochemical experiments. Bio-Rad precast 12% Mini-Protean TGX were used for all SDS-gels. Protein transfer was performed using Trans-Blot SD semi-dry cell on PVDF membrane. Rabbit antibodies sc-389-$G\alpha_{t1}$, sc-15382-rhodopsin were from Santa Cruz Biotechnology (Santa Cruz, CA). Mouse FLAG M2 F1804 were from Sigma-Aldrich. Rabbit HA TA150084 were from Origene. Rabbit PDE6A PA1-720, PDE6G PA1-723 and beta Actin PA1-16889 and secondary HRP antibodies were from Invitrogen. Rabbit antibodies against $G\beta_1$ and $G\gamma_1$ were a gift from N. Gautam (Washington University, St. Louis, MO). Primary antibody dilution was 1:1,000. Secondary antibody dilution was 1:10,000. All gels/blots were developed and analyzed in compliance with the digital image and integrity policies. Prior to blocking non-specific binding by 5% BSA in TBST, the PVDF membranes were cut to size using Amersham Rainbow molecular weight markers as a guide. For proteins with significantly different molecular weights, such as $G\alpha_{t1}$ and $G\gamma_1$, the membrane

was cut in half horizontally into the upper and lower portions, which were stained with individual antibodies. After staining with primary and secondary antibodies, blots were developed using Amersham ECL Prime detection kit. Chemiluminescence was visualized using Li-COR C-DiGit® Blot Scanner that was setup to collect and save time-lapse data in the high-sensitivity mode. Quantitation was performed using Image Studio software. The pixel saturation tool was used to ensure that optical density (OD) of protein bands is not saturated, and only unsaturated bands in a linear range of protein band intensities were used for quantitation. Local background was subtracted.

## Light microscopy and immunohistochemistry

For immune labeling, eyes were cryo-preserved in Tissue-Tek O.C.T. compound. Semi-thin 0.9-μm sections were cut in the dorsal-to-ventral direction through the optic nerve and immunostained as previously described [20]. Images were taken on a Leica DM 5500 D microscope using DFC360 FX camera.

For the $G\alpha_{t1}$ translocation experiment, mice were dark-adapted overnight, their eyes were dilated with one drop of 1% atropine sulfate and then exposed for 15 minutes to steady white background light of various intensities, measured by Sper Scientific Advanced Light Meter 840022, followed by euthanasia by $CO_2$ and eye cryo-preservation. Unsaturated pictures of cross-sections of the retina immunolabelled with anti-$G\alpha_{t1}$ antibody were analyzed in Adobe Photoshop CS4 Extended using the analysis module. Integrated density (ID) was measured in the rod outer segment (OS), and combined area of rod inner segment (IS), rod outer nuclear layer (ONL) and outer plexiform layer (OPL) in three independent sections. $ID_{OS}+(ID_{IS}+OD_{ONL}+OD_{OPL})$ was taken as 100% followed by the calculation of the proportion of $G\alpha_{t1}$ in OS as $ID_{OS}$ in percent.

## *In vivo* electroretinography (ERG)

Animals were dark-adapted overnight and anesthetized by subcutaneous injection of ketamine (80 mg/kg) and xylazine (15 mg/kg). Pupils were dilated with 1% atropine sulfate. During testing, a heating pad controlled by a rectal temperature probe maintained body temperature at 37–38˚C. Full-field ERGs were recorded using a UTAS BigShot apparatus (LKC Technologies) and corneal cup electrodes, as described [21]. The reference electrode needle was inserted under the skin at the skull. Test flashes of white light ranging from $2.5x10^{-5}$ cd·s $m^{-2}$ to 700 cd·s $m^{-2}$ were applied in darkness (scotopic conditions). Responses from several trials were averaged and the intervals between trials were adjusted so that responses did not decrease in amplitude over the series of trials for each step. The recorded responses were low-pass filtered at 500 Hz.

## Single-cell suction recordings

Mice were dark-adapted overnight, sacrificed by $CO_2$ asphyxiation, and their retinas were removed under infrared illumination. Retinas were chopped into small pieces with a razor blade and transferred to a perfusion chamber on the stage of an inverted microscope. A single rod outer segment on the edge of a retina piece was drawn into a glass microelectrode filled with solution containing 140 mM NaCl, 3.6 mM KCl, 2.4 mM $MgCl_2$, 1.2 mM $CaCl_2$, 3 mM HEPES (pH 7.4), 0.02 mM EDTA, and 10 mM glucose. The perfusion solution contained 112.5 mM NaCl, 3.6 mM KCl, 2.4 mM $MgCl_2$, 1.2 mM $CaCl_2$, 10 mM HEPES (pH 7.4), 20 mM $NaHCO_3$, 3 mM Na succinate, 0.5 mM Na glutamate, 0.02 mM EDTA, and 10 mM glucose. The solution was bubbled with 95% $O_2$ / 5% $CO_2$ mixture and its temperature was maintained at 37˚C with an in-line ceramic heater.

Rods were stimulated with 20-ms test flashes of calibrated 500 nm light. The light intensity was controlled with neutral density filters in 0.5 log unit steps. Photoresponses were amplified, low-pass filtered (30 Hz, 8-pole Bessel), and digitized (1 kHz). Data were analyzed using Clampfit 10.6 and Origin 8.5 software. Intensity-response relationships were fitted with Naka-Rushton hyperbolic function:

$$R = \frac{R_{max} \cdot I^n}{I^n + I_{1/2}^n}, \quad (1)$$

where $R$ is the transient-peak amplitude of the rod response, $R_{\max}$ is the maximal response amplitude, $I$ is the flash intensity, $n$ is the Hill coefficient (exponent), and $I_{1/2}$ is the half-saturating light intensity. Normalized rod flash sensitivity ($S_f$) was calculated from the linear part of the intensity-response curve, as follows:

$$S_f = \frac{R}{R_{max} \cdot I}, \quad (2)$$

where $R$ is the amplitude of dim flash response, $R_{max}$ is the maximal response amplitude for that cell, and $I$ is the flash strength used to elicit the dim flash response.

The amplification of the rod phototransduction cascade was evaluated from test flash intensities that produced identical rising phases of dim flash responses. This approach was preferred to calculation of the amplification constant by the method of Lamb and Pugh [22], due to the relatively long duration of test flashes and the effect of low-pass filtering on the response front. Integration time ($T_{\text{integr.}}$) was calculated as the integral of the dim flash response with the transient peak amplitude normalized to unity. The time constant of the dim flash response recovery ($\tau_{\text{rec}}$) was derived from single-exponential fit to the falling phase of the response. The dominant recovery time constant ($\tau_{\text{D}}$) was determined from supersaturating flashes [23], using a 10% criterion for recovery of the photocurrent from saturation.

## Transretinal ERG recordings

Mice were dark-adapted overnight and sacrificed by $CO_2$ asphyxiation. The whole retina was removed from each mouse eyecup under infrared illumination and stored in oxygenated aqueous L15 (13.6 mg/ml, pH 7.4) solution (Sigma-Aldrich) containing 0.1% BSA, at RT. The retina was mounted on filter paper with the photoreceptor side up and placed in a perfusion chamber [24] between two electrodes connected to a differential amplifier. The tissue was perfused with bicarbonate-buffered Locke's solution supplemented with 2 mM L-glutamate and 10 μM DL-2-amino-4-phosphonobutyric acid to block postsynaptic components of the photoresponse [25], and with 20 μM $BaCl_2$ to suppress the slow glial PIII component [26]. The perfusion solution was continuously bubbled with a 95% $O_2$ / 5% $CO_2$ mixture and heated to 36–37˚C.

The photoreceptors in the retina were stimulated with 20-ms test flashes of calibrated 505 nm LED light. The light intensity was controlled by a computer in 0.5 log unit steps. The prolonged (> 1 h) background illumination was achieved with the same 505 nm LED activating ~830 rhodopsin molecules ($R^*$) per rod per second initially. Photoresponses were amplified by a differential amplifier (DP-311, Warner Instruments), low-pass filtered at 30 Hz (8-pole Bessel), and digitized at 1 kHz. Data were analyzed with Clampfit 10.6 and Origin 8.5 software.

## Statistical analysis

For all experiments, data were expressed as mean ± SEM and analyzed with the independent two-tailed Student's $t$-test (using an accepted significance level of $p < 0.05$).

## Results

### Generation of the three transgenic Gγ lines

The transgenic mice were generated using the construct shown in Fig 2. We used the mouse opsin promoter to target the expression of each of the three transgenic Gγ subunits selectively in rod photoreceptors. We also included a 3xFLAG and an HA tag to facilitate detection of the transgenic protein in the retina. Upon the successful generation of the three $G\gamma_1$, $G\gamma_c$, and $G\gamma_{11}$ transgenic strains, we crossed them with the rod $G\gamma_1$-deficient (*Gngt1*$^{-/-}$) line to effectively substitute the rod $G\gamma_1$ with each of the transgenic Gγ subunits. As we have shown previously, deletion of rod $G\gamma_1$ in mice results in dramatic suppression of rod sensitivity and reduction in the expression of the other two rod transducin subunits, $G\alpha_{t1}$ and $G\beta_1$ [2], see also [3]. Thus, generating *Gγ*$_1$$^{+}$*Gngt1*$^{-/-}$, *Gγ*$_c$$^{+}$*Gngt1*$^{-/-}$, and *Gγ*$_{11}$$^{+}$*Gngt1*$^{-/-}$ mice allowed us to investigate how the substitution of the endogenous rod $G\gamma_1$ subunit with transgenic $G\gamma_1$ (as a control), or with $G\gamma_c$ or $G\gamma_{11}$ will affect the Gt expression profile and functional properties of mouse rods.

We began our analysis by investigating the expression localization of the $G\gamma_1$, $G\gamma_c$, and $G\gamma_{11}$ γ-subunits in their respective transgenic mouse retinas. To prevent light-driven translocation and ensure that all Gt subunits were properly localized in the outer segments of rods, these experiments were performed after dark-adapting the animals overnight. Using an anti-FLAG antibody staining of retinal sections, we found, as expected, that no transgenic protein was found in wild type or *Gngt1*$^{-/-}$ retinas (Fig 3A and 3B). Transgenic $G\gamma_1$, $G\gamma_c$, and $G\gamma_{11}$ subunits were all, indeed, localized in the outer segments of rods (Fig 3C–3E). Thus, in addition to the transgenically reintroduced $G\gamma_1$, both cone $G\gamma_c$ and the non-photoreceptor $G\gamma_{11}$ were targeted properly to the rod outer segments following dark adaptation.

The level of transducin in rod outer segments is directly proportional to the amplification of rod phototransduction [27], making its proper translocation crucial for the function of rods. Our finding that all three transgenic Gγ subunits localized properly to the rod outer segments was critical for enabling us to perform the subsequent physiological analysis of the three transgenic mouse lines and to compare directly their functional properties. Notably, our immunohistochemical analysis also showed that all three transgenic lines retained normal retina morphology and uniform expression of the transgenic proteins in the $G\gamma_1$-deficient rods.

### Restoration of transducin complement in all Gγ-expressing lines

Quantitative Western blot analysis was performed in the linear portion of the dose escalation plots of the total retina protein vs. optical densities of the protein bands to assure the Western

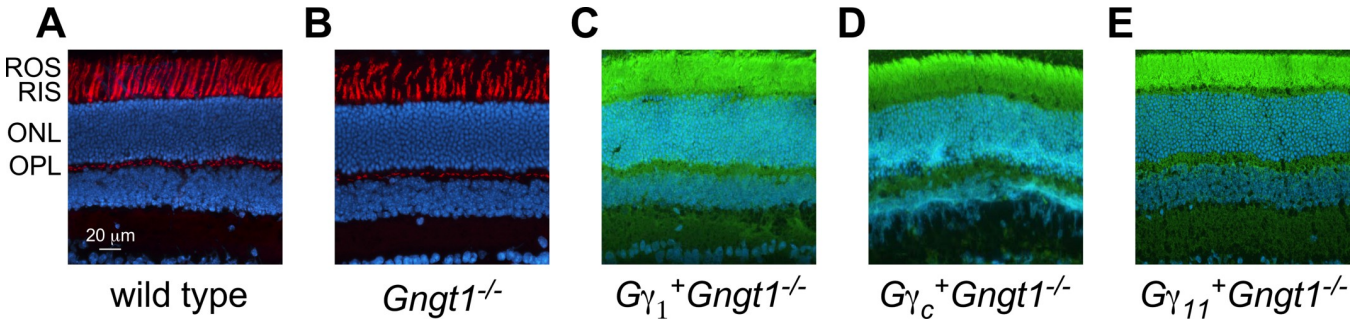


**Fig 3. Immunohistochemical analysis of the transgenic protein expression using anti-FLAG antibodies (green), with DAPI counterstaining (blue), at P30.** (**A**) and (**B**) are also counterstained with wheat germ agglutinin (red) to highlight ROS/RIS. Cryo-sections, 40x. (**A**) wild type, (**B**) *Gngt1*$^{-/-}$, (**C**) *Gγ*$_1$$^{+}$*Gngt1*$^{-/-}$, (**D**) *Gγ*$_c$$^{+}$*Gngt1*$^{-/-}$, (**E**) *Gγ*$_{11}$$^{+}$*Gngt1*$^{-/-}$ retinas. ROS–rod outer segments, RIS–rod inner segments, ONL–outer nuclear layer, OPL–outer plexiform layer.

https://doi.org/10.1371/journal.pone.0272506.g003

signal is not saturated, typically in the 5–20 μg range. It showed that expression levels of general cellular protein actin and rhodopsin in the retina were comparable in $G\gamma_1{}^{+}Gngt1^{-/-}$, $G\gamma_c{}^{+}Gngt1^{-/-}$, and $G\gamma_{11}{}^{+}Gngt1^{-/-}$ mice (Fig 4A and 4B), a finding consistent with the normal morphology and lack of degeneration in these retinas (Fig 3). Direct protein expression comparison in Fig 4C used 10 μg of retina protein in each sample. $G\gamma_1$, $G\gamma_c$, and $G\gamma_{11}$ transgenic proteins were easily identified by both anti-FLAG and anti-HA staining (Fig 4C). Expression levels of the three γ-subunits also appeared similar by this test. $G\gamma_1$-specific antibodies stained transgenic $G\gamma_1$ stronger, compared to the native $G\gamma_1$ in WT samples (Fig 4C, bottom), which may be explained either by higher level of transgenic protein whose expression is driven by the strong *rhodopsin* promoter compared to the *Gngt1* promoter in wild type retinas, or possibly by better accessibility of the N-terminal epitope in the transgenic protein. Western blots also showed that expression of each of the transgenic Gγ subunits restores the amounts of $G\alpha_{t1}$ to wild type levels (Fig 4C). Restoration of $G\alpha_{t1}$ expression in all transgenic lines was also corroborated by the robust staining and proper $G\alpha_{t1}$ localization to the rod outer segments in dark adapted retinas, discussed separately in Fig 8. The expression levels of $G\beta_1$ were also recovered (Fig 4C). As expected, all three transgenic retinas expressed equal amounts of the effector protein PDE6, as judged by the similar intensities of protein bands for PDE6α and PDE6γ

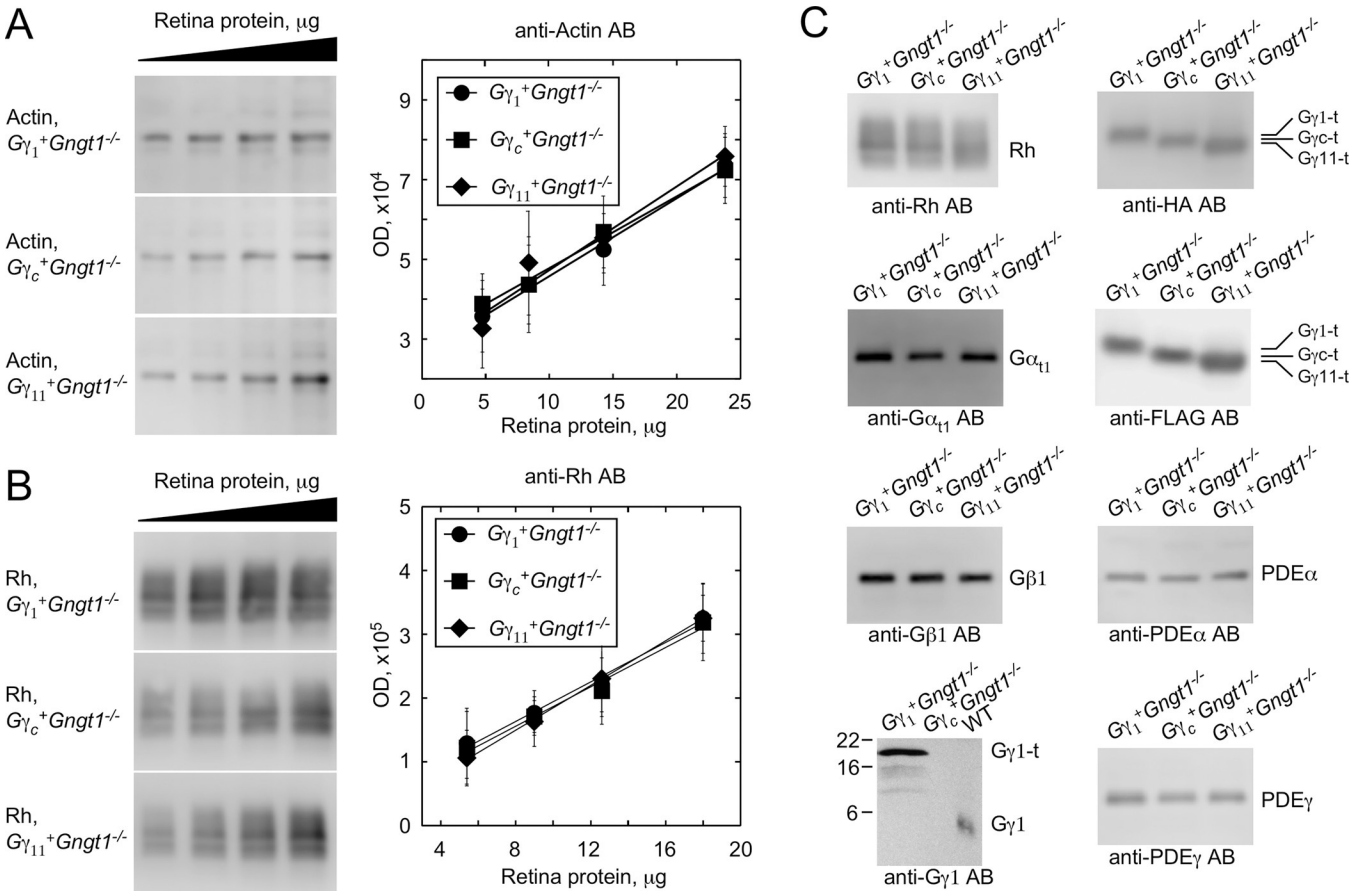


**Fig 4. Western blot analysis of retina homogenates obtained from indicated transgenic mice.** Representative staining for actin (**A**) and rhodopsin (**B**) in samples with progressively increasing amounts of loaded retina homogenate obtained from $G\gamma_1{}^{+}Gngt1^{-/-}$, $G\gamma_c{}^{+}Gngt1^{-/-}$, and $G\gamma_{11}{}^{+}Gngt1^{-/-}$ mice. Graph shows optical density of Western blot bands against amount of total retina protein (n = 3). Linearity of plots demonstrates sub-saturating ECL signal ensuring direct quantitative comparison. (**C**) Comparative staining of samples from the $G\gamma_1{}^{+}Gngt1^{-/-}$, $G\gamma_c{}^{+}Gngt1^{-/-}$, and $G\gamma_{11}{}^{+}Gngt1^{-/-}$ retina homogenates using indicated antibodies against rhodopsin, $G\alpha_{t1}$, $G\beta_1$, $G\gamma_1$, HA, FLAG, PDEα, and PDEγ subunits.

https://doi.org/10.1371/journal.pone.0272506.g004

(Fig 4C). Thus, transgenic retinas appeared to express the full and equal sets of rhodopsin, transducin, and PDE.

## Restoration of scotopic visual function in all Gγ-expressing lines

To determine how the expression of each of the three Gγ-subunits affects the functional properties of rods, we first performed electroretinography (ERG) analysis of control wild type and *Gngt1*$^{-/-}$ mice and the transgenic *Gγ*$_1$$^{+}$*Gngt1*$^{-/-}$, *Gγ*$_c$$^{+}$*Gngt1*$^{-/-}$, and *Gγ*$_{11}$$^{+}$*Gngt1*$^{-/-}$ mice *in vivo* (Fig 5A–5E). As we have previously shown [2], deletion of the rod Gγ$_1$-subunit results in substantial desensitization and reduction in the maximal ERG a-wave response (Fig 5F, open light grey circles). Notably, expression of Gγ$_1$, Gγ$_c$, or Gγ$_{11}$ in the *Gngt1*$^{-/-}$ mice (Fig 5F, filled

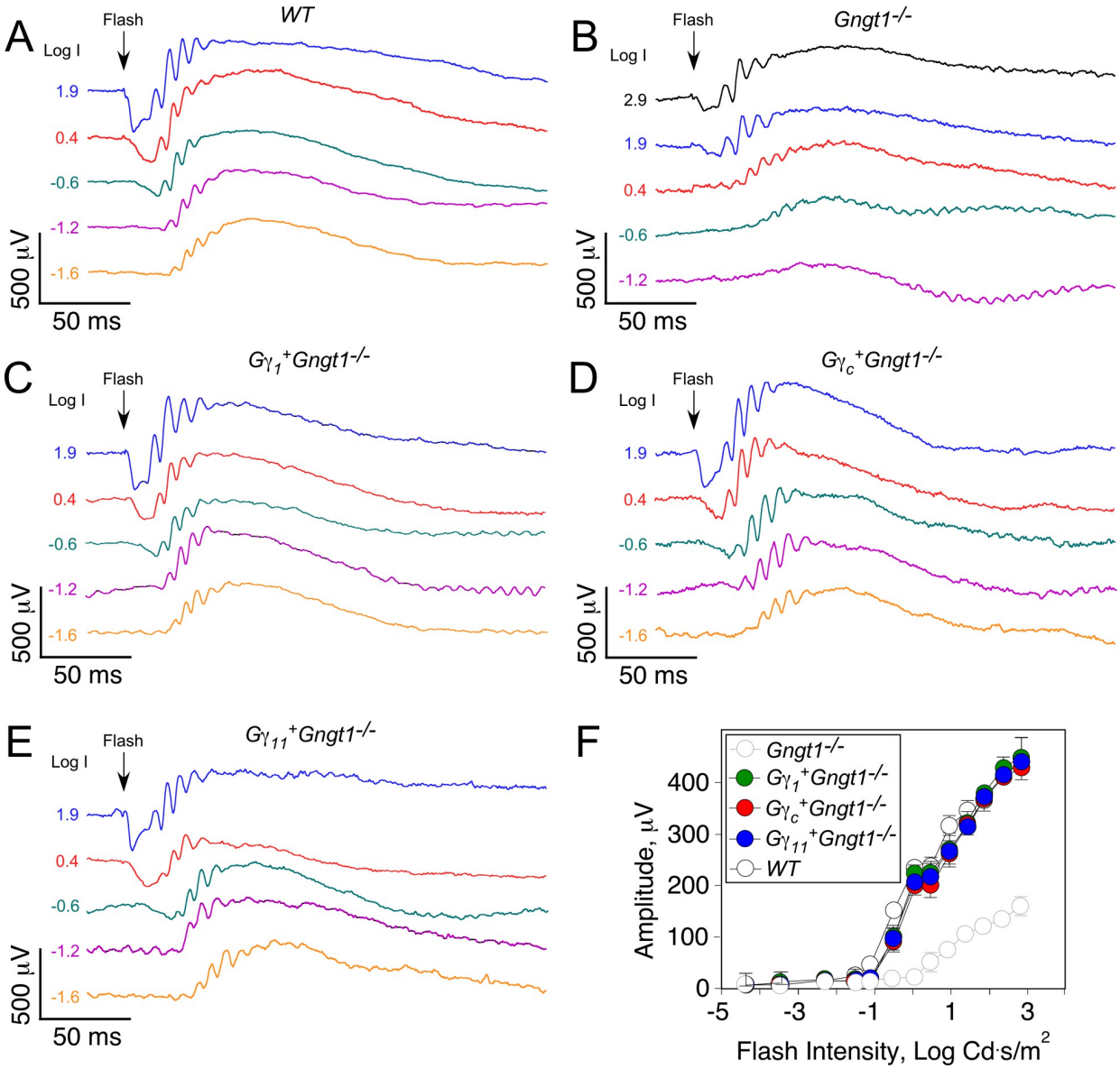


**Fig 5.** Families of *in vivo* ERG responses from wild type **(A)**, *Gngt1*$^{-/-}$ **(B)**, *Gγ*$_1$$^{+}$*Gngt1*$^{-/-}$ **(C)**, *Gγ*$_c$$^{+}$*Gngt1*$^{-/-}$ **(D)**, and *Gγ*$_{11}$$^{+}$*Gngt1*$^{-/-}$ **(E)** mice. Waveforms are color coded according to the white flash of indicated intensity. **(E)** Averaged scotopic *in vivo* ERG intensity-response functions (mean ± SEM) for wild type (n = 3), *Gngt1*$^{-/-}$ (n = 3), *Gγ*$_1$$^{+}$*Gngt1*$^{-/-}$ (n = 3), *Gγ*$_c$$^{+}$*Gngt1*$^{-/-}$ (n = 3), and *Gγ*$_{11}$$^{+}$*Gngt1*$^{-/-}$ (n = 3) mouse lines.

https://doi.org/10.1371/journal.pone.0272506.g005

circles) all restored robust scotopic function essentially to the wild type level (Fig 5F, open black circles; see also [28] for the reference to wild type data). Thus, not only did the transgenic expression of $G\gamma_1$ rescue scotopic vision in the $G\gamma_1$-deficient mice, but the same effect could be achieved by expressing the cone $G\gamma_c$ or the non-photoreceptor $G\gamma_{11}$.

## Restoration of rod photosensitivity and response kinetics in all Gγ-expressing lines

Next, we analyzed by suction electrode recordings whether the transgenic expression of the three different Gγ-subunits in individual *Gngt1*$^{-/-}$ mouse rods would restore their photosensitivity and response kinetics. In agreement with the similar length of their outer segments at the age of 4–5 weeks (Fig 2) and normal ERG responses *in vivo* (Fig 5), $G\gamma_1$$^{+}$*Gngt1*$^{-/-}$, $G\gamma_c$$^{+}$*Gngt1*$^{-/-}$, and $G\gamma_{11}$$^{+}$*Gngt1*$^{-/-}$ rods produced saturated responses of similar amplitudes, not different from these in wild type and *Gngt1*$^{-/-}$ cells (Fig 6A–6F and Table 1). Remarkably, compared to the dramatically desensitized (~70-fold) $G\gamma_1$-deficient rods, the light sensitivity of all transgenic photoreceptors was restored to wild type levels (Fig 6F). It should be noted, however, that the average sensitivity of $G\gamma_{11}$$^{+}$*Gngt1*$^{-/-}$ rods was slightly (~20%) higher than that in the other two Gγ-expressing lines (Table 1).

We then evaluated the kinetics of activation of the rod phototransduction cascade in all three mutant mouse strains by directly comparing the light intensities required to produce identical initial phases of response activation (Fig 7A). In accordance with their restored sensitivity, the phototransduction amplification in $G\gamma_1$$^{+}$*Gngt1*$^{-/-}$ rods was increased by ~34-fold compared to that in cells lacking $G\gamma_1$ and reached wild type level, as evident from the analysis of rising phases of their dim flash responses during the first 40 ms after the test flash. The cascade activation was only slightly (~10%) lower in $G\gamma_c$$^{+}$*Gngt1*$^{-/-}$ rods and higher (by ~10%) in $G\gamma_{11}$$^{+}$*Gngt1*$^{-/-}$ cells than in the $G\gamma_1$-expressing transgenic rods, thus showing a comparable degree of restoration in all three transgenic lines.

One characteristic feature of *Gngt1*$^{-/-}$ rods is the significantly faster inactivation of their signaling cascade, an effect contributing to their reduced photosensitivity [2]. In contrast, normal inactivation rate of dim flash responses was achieved in the rods of all transgenic lines expressing a Gγ-subunit, as judged from their normal time-to-peak, integration time, and single-exponential dim flash response recovery time constant ($\tau_{rec}$) (Fig 7B and Table 1). Coincidentally, the response recovery following supersaturating flashes was also slower in all transgenic lines than in $G\gamma_1$-deficient controls, as evident from comparing the kinetics of their maximal rod responses (Fig 7C) and the corresponding dominant recovery time constants ($\tau_D$) (Fig 7D and Table 1). All these parameters were also comparable to those typically observed in wild type mouse rods (Table 1 and [2]). It should be mentioned that the rods expressing $G\gamma_{11}$ had the slowest $\tau_D$ among all transgenic cells (Table 1) although the molecular mechanisms behind their slight response deceleration remain unclear. Taken together, these results indicate that the transgenic expression of various G-protein γ-subunits with distinct amino acid sequences rescues equally well the expression level of rod transducin α-subunit in $G\gamma_1$-deficient mouse rods and effectively restores their signaling, although with slightly different photoresponse kinetics.

## Light-driven translocation of $Gt\alpha_1$ in Gγ-expressing rods

Finally, we investigated how the expression of each of the three transgenic Gγ subunits in rods affects the light-driven translocation of $G\alpha_{t1}$ from the outer segment to the inner segment of these photoreceptors. We examined the distribution of $G\alpha_{t1}$ across the rods in 5 different background light conditions: darkness and at 1, 10, 100, and 1000 lux of steady background

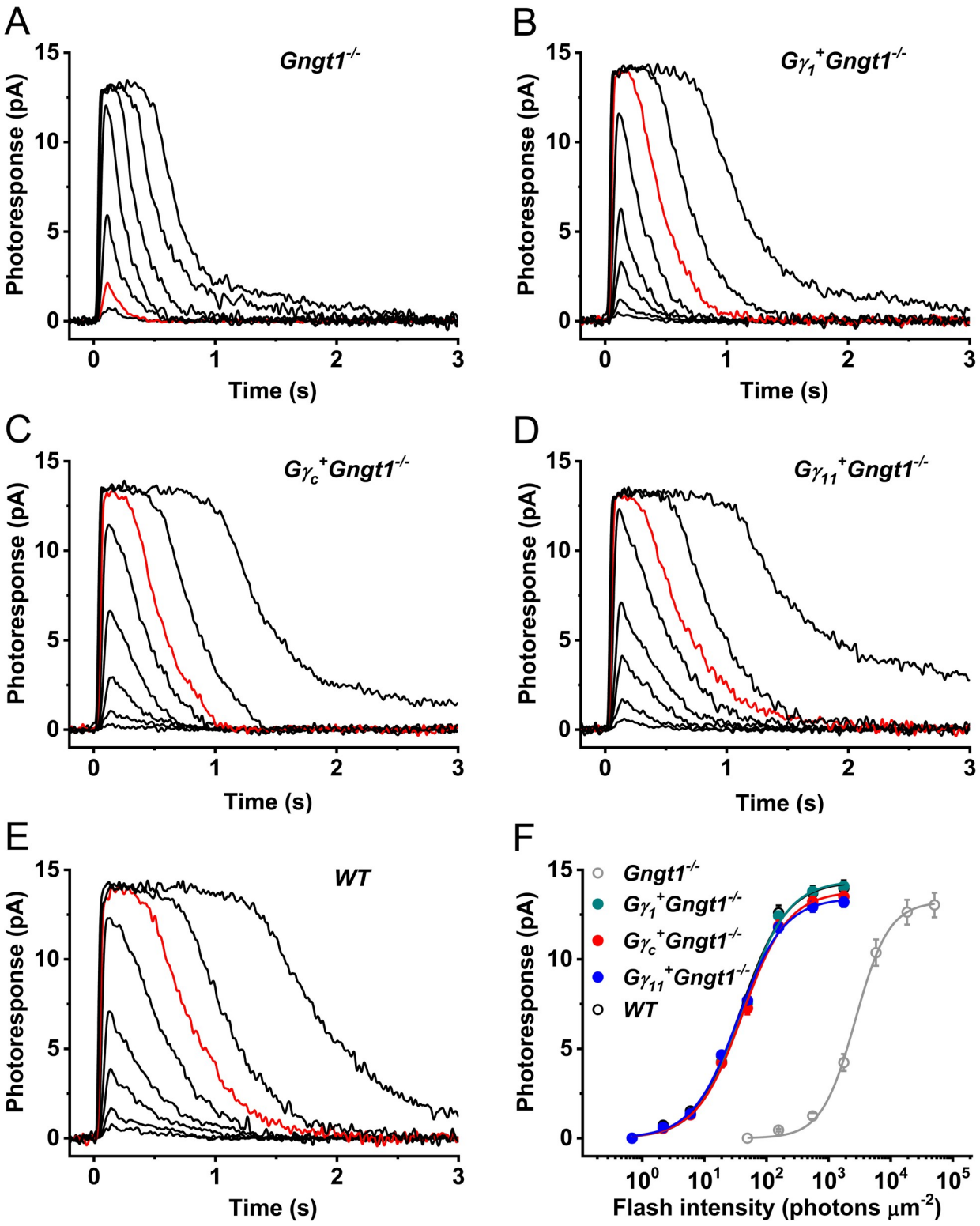


**Fig 6. Light responses of rods in control and transgenic mouse lines expressing different Gγ-subunits.** (**A–E**) Representative families of flash responses from 4–5-week-old control *Gngt1*$^{-/-}$ (**A**), *Gγ*$_1$$^{+}$*Gngt1*$^{-/-}$ (**B**), *Gγ*$_c$$^{+}$*Gngt1*$^{-/-}$ (**C**), *Gγ*$_{11}$$^{+}$*Gngt1*$^{-/-}$ (**D**), and wild type (**E**) mouse rods. Test flashes of 500 nm light with intensities of 160, 560, 1.8x10$^3$, 5.8x10$^3$, 1.8x10$^4$, 5.1x10$^4$, and 1.6x10$^5$ photons μm$^{-2}$ (for *Gngt1*$^{-/-}$ rods) or 2, 6, 19, 50, 160, 560, 1.8x10$^3$, and 5.8x10$^3$ photons μm$^{-2}$ (for wild type and all transgenic rods) were delivered at time 0. Red traces show responses to identical light intensity (560 photons μm$^{-2}$). (**F**) Averaged intensity-response relationships (mean ± SEM) for *Gngt1*$^{-/-}$ (n = 11), *Gγ*$_1$$^{+}$*Gngt1*$^{-/-}$ (n = 31),

$G\gamma_c^+Gngt1^{-/-}$ (n = 30), $G\gamma_{11}^+Gngt1^{-/-}$ (n = 24), and wild type (n = 8) mouse rods. Data were fitted with hyperbolic Naka-Rushton functions that yielded half-saturating light intensities ($I_{1/2}$) indicated in Table 1. Error bars are smaller than the symbol size for most data points.

https://doi.org/10.1371/journal.pone.0272506.g006

illumination. To allow translocation to occur, dark-adapted animals were exposed to the background light for 15 minutes, and then were rapidly euthanized and their eyes were dissected, cryo-preserved, sectioned, and stained with the $G\alpha_{t1}$ antibody for immunohistochemical

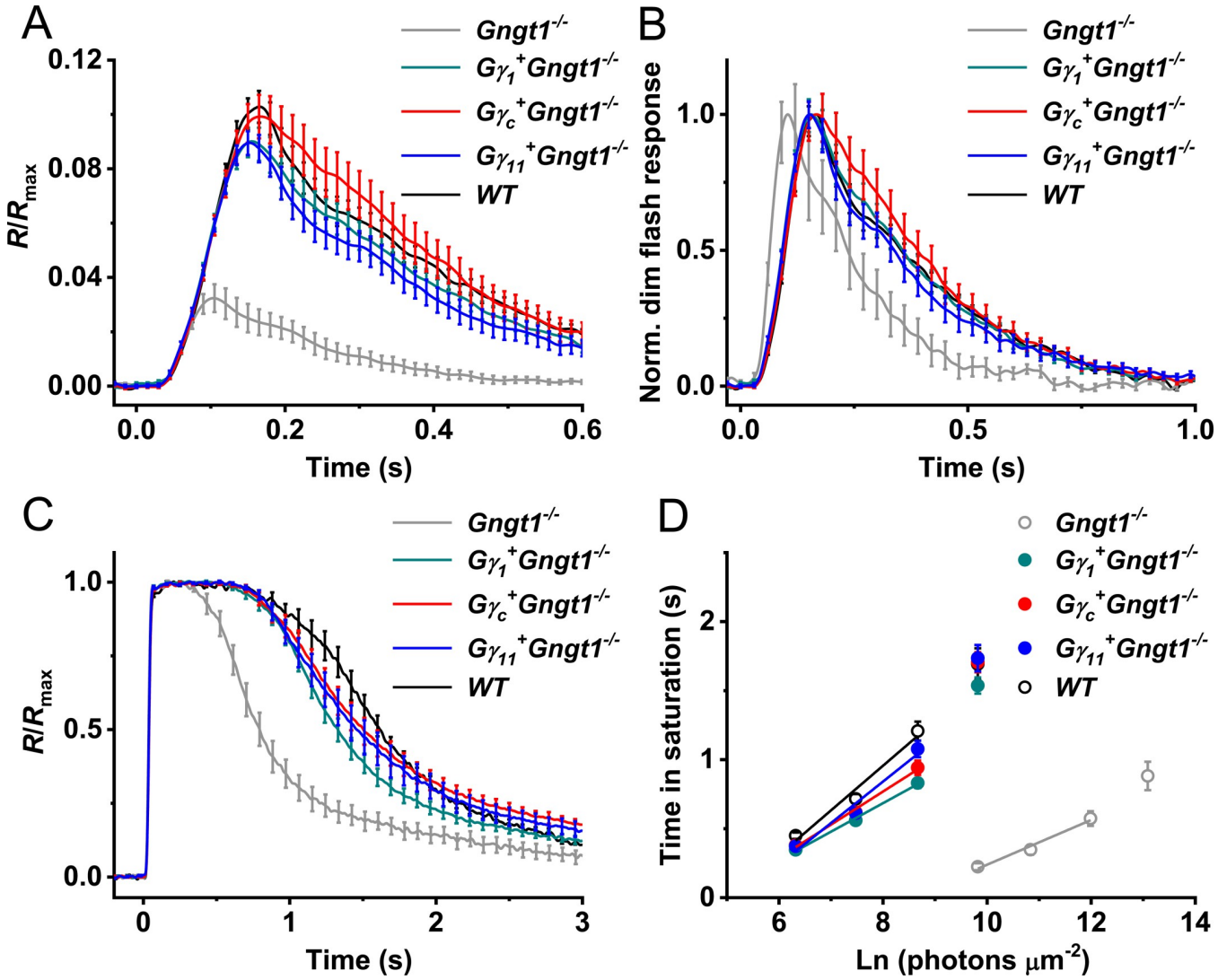


**Fig 7. Activation and inactivation of rod phototransduction cascade in control and transgenic mice expressing different Gγ subunits.** (**A**) Amplification of phototransduction in mouse rods. Dim flash responses (to light intensities of 560 photons $\mu m^{-2}$ for $Gngt1^{-/-}$ rods and 6 photons $\mu m^{-2}$ for wild type and all transgenic Gγ-expressing rods) were normalized to maximum dark currents ($R_{max}$) of the respective cells and population-averaged (mean ± SEM). Then, the $Gngt1^{-/-}$, $G\gamma_c^+Gngt1^{-/-}$, and $G\gamma_{11}^+Gngt1^{-/-}$ responses were scaled to make their initial rising phase to coincide with that of the wild type response. Correspondingly scaled light intensities were 0.03:1:0.9:1.1:1 ($Gngt1^{-/-}$:$G\gamma_1^+Gngt1^{-/-}$:$G\gamma_c^+Gngt1^{-/-}$:$G\gamma_{11}^+Gngt1^{-/-}$:*WT*), indicating ~30-fold higher gain in the Gγ-expressing rods. (**B**) Phototransduction shutoff in mouse rods. Dim flash responses (to light intensities of 560 photons $\mu m^{-2}$ for control $Gngt1^{-/-}$ rods and 6 photons $\mu m^{-2}$ for wild type and all Gγ-expressing rods) were normalized to their own maximums and population-averaged (mean ± SEM). (**C**) Supersaturated responses (to light intensities of $1.6x10^5$ photons $\mu m^{-2}$ for control $Gngt1^{-/-}$ rods and $5.8x10^3$ photons $\mu m^{-2}$ for wild type and all Gγ-expressing rods) were normalized to their amplitudes ($R_{max}$) and population-averaged (mean ± SEM). (**D**) Determination of the dominant recovery time constant ($\tau_D$) from a series of supersaturating flashes for $Gngt1^{-/-}$ (n = 11), $G\gamma_1^+Gngt1^{-/-}$ (n = 31), $G\gamma_c^+Gngt1^{-/-}$ (n = 30), $G\gamma_{11}^+Gngt1^{-/-}$ (n = 23), and wild type (n = 8) mouse rods. Linear fits yielded $\tau_D$-values indicated in Table 1. Values are means ± SEM (smaller than the symbol size for some data points).

https://doi.org/10.1371/journal.pone.0272506.g007

**Table 1. Parameters of single-cell responses from dark-adapted mouse rods.**

| Response parameter | *Gngt1*$^{-/-}$ (n = 11) | *Gγ*$_1$$^{+}$*Gngt1*$^{-/-}$ (n = 31) | *Gγ*$_c$$^{+}$*Gngt1*$^{-/-}$ (n = 30) | *Gγ*$_{11}$$^{+}$*Gngt1*$^{-/-}$ (n = 24) | *WT* (n = 8) |
|---|---|---|---|---|---|
| $R_{max}$ (pA) | 13.2 ± 0.6 NS | 14.1 ± 0.3 NS | 13.5 ± 0.3 NS | 13.2 ± 0.3 NS | 14.0 ± 0.4 |
| $T_{peak}$ (ms) | 108 ± 6 *** | 153 ± 4 NS | 162 ± 5 NS | 152 ± 3 NS | 157 ± 5 |
| $T_{integr.}$ (ms) | 177 ± 18 *** | 286 ± 17 NS | 290 ± 15 NS | 278 ± 17 NS | 297 ± 19 |
| $S_f$ (μm$^2$ ph$^{-1}$) | 1.7x10$^{-4}$ ± 2.0x10$^{-5}$ *** | 1.6x10$^{-2}$ ± 8.9x10$^{-4}$ NS | 1.6x10$^{-2}$ ± 1.1x10$^{-3}$ NS | 1.7x10$^{-2}$ ± 1.2x10$^{-3}$ NS | 1.7x10$^{-2}$ ± 1.0x10$^{-3}$ |
| $I_{1/2}$ (ph μm$^{-2}$) | 3007 ± 308 *** | 45 ± 2 NS | 46 ± 3 NS | 38 ± 2 NS | 40 ± 3 |
| $\tau_{rec}$ (ms) | 146 ± 13 ** | 223 ± 16 NS | 214 ± 14 NS | 226 ± 16 NS | 236 ± 13 |
| $\tau_D$ (ms) | 162 ± 15 *** | 207 ± 11 ** | 240 ± 15 * | 301 ± 16 NS | 324 ± 17 |

$R_{max}$, maximal dark current measured from saturated responses; time-to-peak ($T_{peak}$), integration time ($T_{integr.}$), and normalized flash sensitivity ($S_f$) refer to responses whose amplitudes were ~0.2·$R_{max}$ and fell within the linear range; $I_{1/2}$, half-saturating light intensity; $\tau_{rec}$, time constant of single-exponential decay of the dim flash response recovery phase; $\tau_D$, dominant time constant of recovery after supersaturating flashes determined from the linear fit to time in saturation vs. intensity semilog (Pepperberg) plots [23]. Data are presented as mean ± SEM. Student's t-test, NS (not significant) indicates $p > 0.05$

* indicates $p < 0.05$

** indicates $p < 0.01$

*** indicates $p < 0.001$, all compared to wild type values.

https://doi.org/10.1371/journal.pone.0272506.t001

analysis of its distribution. Consistent with the localization of the transgenic Gγ$_1$, Gγ$_c$, and Gγ$_{11}$ subunits to the outer segments of rods in dark-adapted retinas (Fig 3), we found that Gα$_{t1}$ was also properly localized in the rod outer segments in darkness (0 lux; Fig 8A–8C, left panels, and 8D). In *Gγ*$_1$$^{+}$*Gngt1*$^{-/-}$ and *Gγ*$_c$$^{+}$*Gngt1*$^{-/-}$ mice, approximately 90% of Gtα$_{t1}$ remained in the outer segments in dim background illumination of 1 and 10 lux, and eventually translocated to the inner segments when the retinas were illuminated with 100 and 1000 lux of light (Fig 8A and 8B, right two panels). This is qualitatively consistent with previous work showing that in wild type mouse rods the threshold for transducin translocation is near 4.6x10$^3$ R* rod$^{-1}$ s$^{-1}$ [29], and indistinguishable from the Gtα$_{t1}$ translocation in wild type and *Gngt1*$^{+/-}$ retinas under identical conditions. The *Gngt1*$^{+/-}$ control contains one *Gngt1*-wild type copy and one *Gngt1*$^{-}$ copy and could be used as a closer genetic match for *Gγ*$_1$$^{+}$*Gngt1*$^{-/-}$ containing one copy of the *Gngt1* transgene and two *Gngt1*$^{-}$ copies. In contrast, translocation of Gα$_{t1}$ in *Gγ*$_{11}$$^{+}$*Gngt1*$^{-/-}$ retinas was triggered with illumination as low as 1 lux (Fig 8C and 8D, blue circles). At 1 lux, only 10% of Gα$_{t1}$ remained in the outer segments of the *Gγ*$_{11}$$^{+}$*Gngt1*$^{-/-}$ retinas compared to 90% for the other two Gγ transgenes in respective lines (Fig 8D). The highly robust Gα$_{t1}$ staining in the outer nuclear layer that is evident at 100 and 1000 lux in the *Gγ*$_{11}$$^{+}$*Gngt1*$^{-/-}$ retinas is typically observed in wild type and *Gngt1*$^{+/-}$ controls only at background illumination levels above 1000 lux. Thus, surprisingly, despite the essentially identical functional properties of dark-adapted rods expressing the three transgenic Gγ subunits, translocation of transducin during continuous light exposure was initiated at substantially lower light intensity in transgenic Gγ$_{11}$ rods compared to transgenic Gγ$_1$ or Gγ$_c$ cells.

It was recently shown that the gradual translocation of transducin from the outer to the inner segments of rods under continuous illumination results in partial recovery of the rod response after its initial suppression by the background light [30]. Thus, we sought to determine whether the lower threshold for Gα$_{t1}$ translocation found in *Gγ*$_{11}$$^{+}$*Gngt1*$^{-/-}$ retinas affects the amplitude of the rod response over the course of 1-h exposure to background light. We used transretinal (*ex vivo* ERG) recordings to obtain and monitor the rod-driven responses. We exposed control *Gngt1*$^{+/-}$ and transgenic *Gγ*$_{11}$$^{+}$*Gngt1*$^{-/-}$ retinas to a moderate sub-saturating background light activating ~830 visual pigment molecules (R*) per rod per second at onset. This light would be expected to trigger transducin translocation in Gγ$_{11}$ transgenic retinas but not in control retinas (Fig 8, see also [29]). As expected, in control retinas, the onset of

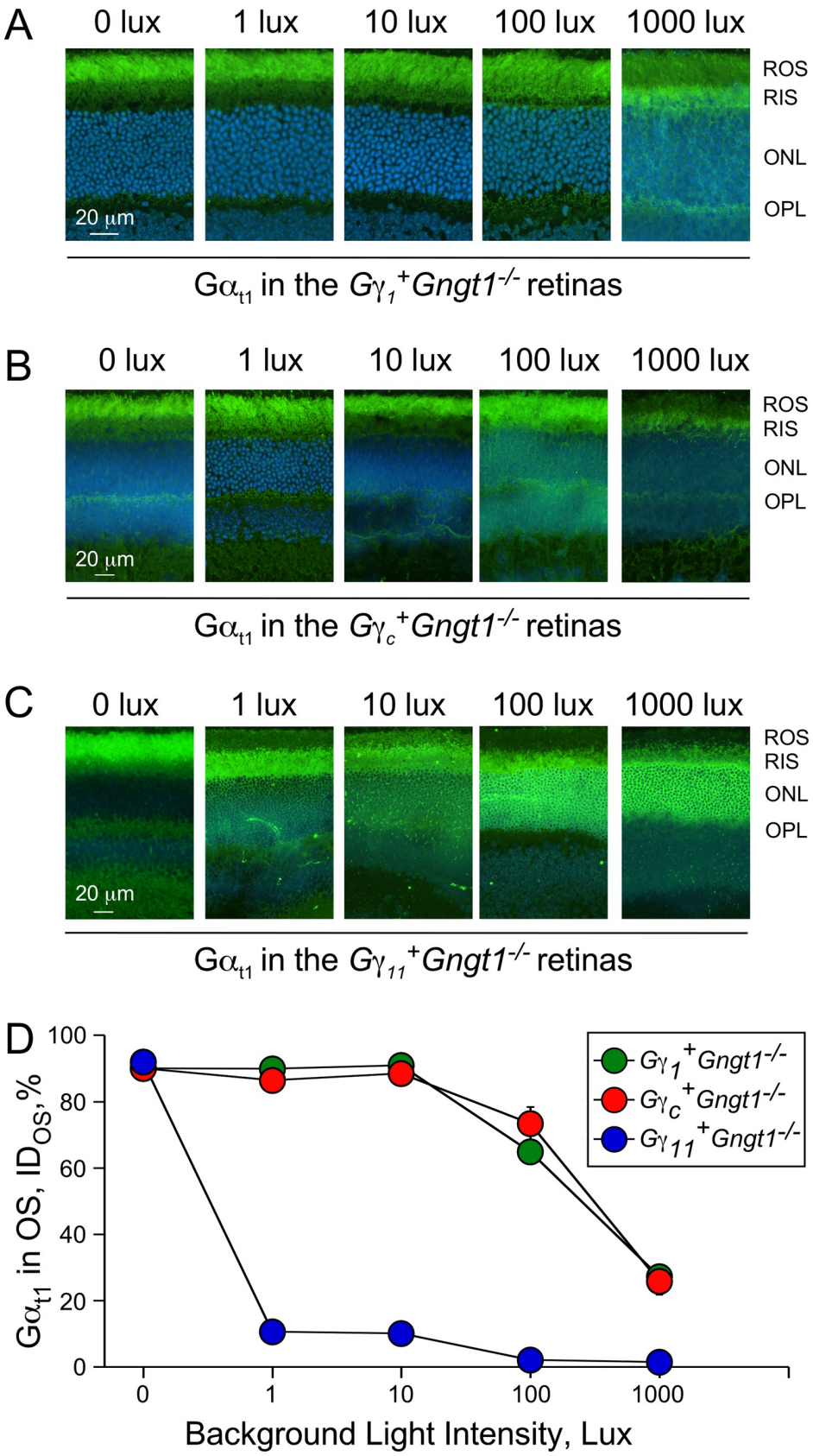
A
0 lux
1 lux
10 lux
100 lux
1000 lux
ROS
RIS
ONL
OPL
20 μm
Gα$_{t1}$ in the Gγ$_1$$^+$Gngt1$^{-/-}$ retinas
B
0 lux
1 lux
10 lux
100 lux
1000 lux
ROS
RIS
ONL
OPL
20 μm
Gα$_{t1}$ in the Gγ$_c$$^+$Gngt1$^{-/-}$ retinas
C
0 lux
1 lux
10 lux
100 lux
1000 lux
ROS
RIS
ONL
OPL
20 μm
Gα$_{t1}$ in the Gγ$_{11}$$^+$Gngt1$^{-/-}$ retinas
D
Gα$_{t1}$ in OS, ID$_{OS}$, %
100
80
60
40
20
0
0
1
10
100
1000
Background Light Intensity, Lux
Gγ$_1$$^+$Gngt1$^{-/-}$
Gγ$_c$$^+$Gngt1$^{-/-}$
Gγ$_{11}$$^+$Gngt1$^{-/-}$

**Fig 8. Translocation of $G\alpha_{t1}$-subunit in $G\gamma$ transgenic retinas under various background light conditions.** Immunohistochemical analysis of retinas stained with anti-$G\alpha_{t1}$ antibody (green) and counterstained with DAPI (blue). $G\alpha_{t1}$ distribution in retinas from the $G\gamma_1^+Gngt1^{-/-}$ (**A**), $G\gamma_c^+Gngt1^{-/-}$ (**B**), and $G\gamma_{11}^+Gngt1^{-/-}$ retinas (**C**). ROS–rod outer segments, RIS–rod inner segments, ONL–outer nuclear layer, OPL–outer plexiform layer. (**D**) Proportion of $G\alpha_{t1}$ in OS vs. IS+ONL+OPL, percent integrated density (n = 3).

https://doi.org/10.1371/journal.pone.0272506.g008

the background light caused a rapid partial suppression of the rod maximal response (Fig 9, black symbols), which then persisted largely unchanged for the 60-min duration of the experiment, only slightly affected by a gradual rundown. The onset of an identical background light in $G\gamma_{11}^+Gngt1^{-/-}$ retinas produced comparable initial suppression of the rod maximal response. However, in stark contrast to the control case, the rod response then gradually recovered over the course of the 60 min of the experiment (Fig 9, blue symbols). As recently argued, this gradual increase reflects the translocation of $G\alpha_{t1}$ away from the rod outer segments, which would effectively reduce the activation of the rod phototransduction by the steady background light,

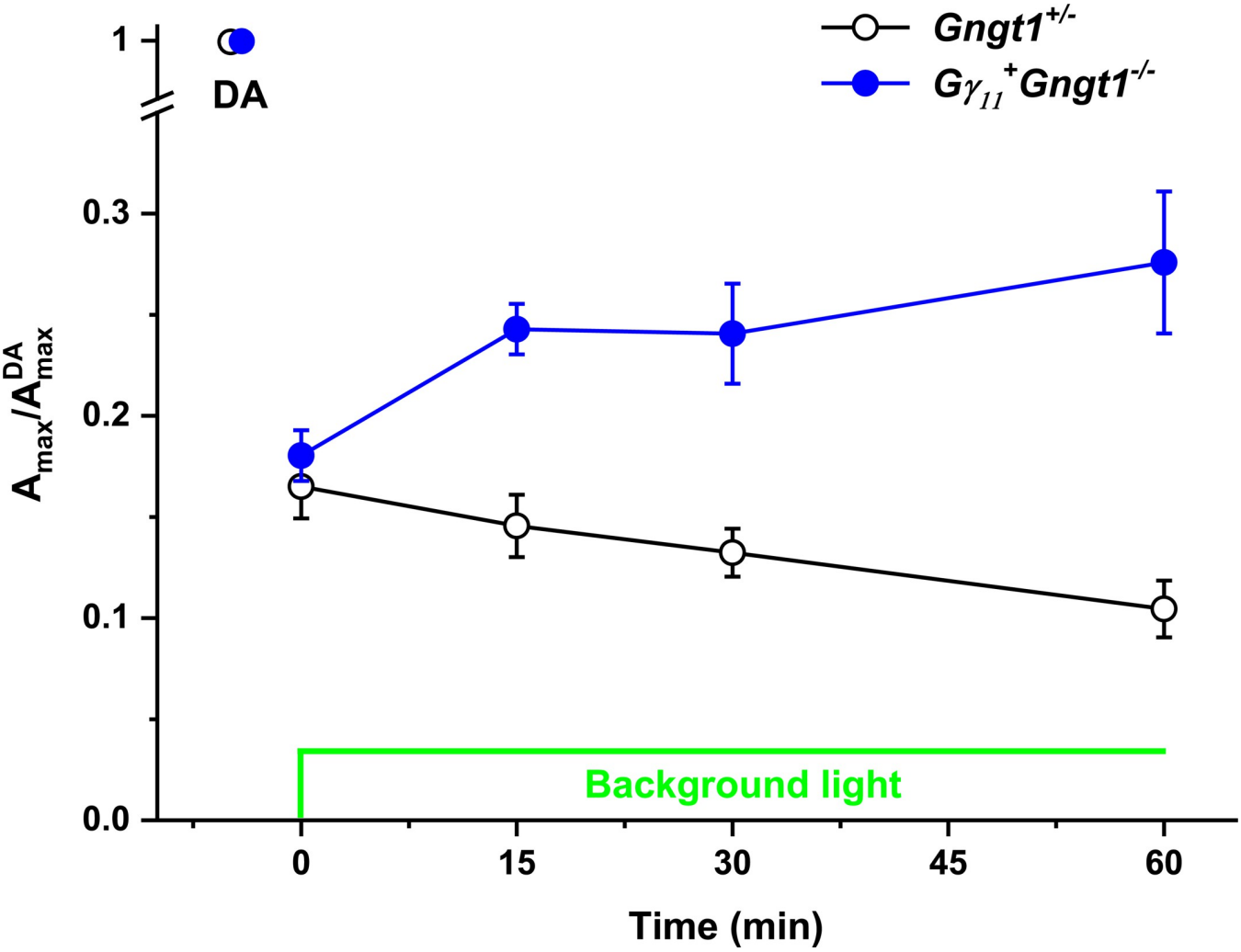


**Fig 9. Changes of rod-driven maximal *ex vivo* transretinal ERG responses in control ($Gngt1^{+/-}$) (n = 4) and transgenic $G\gamma11{+}Gngt1^{-/-}$ (n = 4) retinas.** Retinas were exposed to prolonged moderate non-saturating 505-nm background light activating ~830 visual pigment molecules ($R^*$) per rod per second initially. All maximal responses were normalized to corresponding dark-adapted response amplitudes ($A^{DA}_{max}$) and population-averaged. The onset and duration of background light are shown in green.

https://doi.org/10.1371/journal.pone.0272506.g009

allowing the rods to recover partially their dark current [30]. Thus, the gradual recovery of rod responses in transgenic $G\gamma_{11}^{+}Gngt1^{-/-}$ retinas but not in control retinas in moderate background light is consistent with our observation that in these conditions transducin translocation takes place only in the transgenic $G\gamma_{11}^{+}Gngt1^{-/-}$ rods but not in controls (Fig 8).

## Discussion

Heterotrimeric G-proteins are the main transducers and amplifiers of extracellular signals from GPCRs to the intracellular effectors. It is now firmly established that specificity of the GPCR signaling and fine-tuning of the resulting physiological responses are regulated by the diversity of the Gα subunits, comprised of sixteen family members subdivided into four subfamilies ($G_s$, $G_{i/o}$, $G_{q/11}$, and $G_{12/13}$), as well as by multiple combinations of five Gβ ($G\beta_{1-5}$) and twelve Gγ ($G\gamma_{1-13}$) subunits. In many cell types containing various G-protein combinations, their interplay contributes to the rich gamut of cellular responses with defined spatio-temporal characteristics.

Retinal rod and cone photoreceptors provide a fascinating example of highly specialized sensory neurons that, while employing similar signaling architecture, differ drastically in their light sensitivity, photoresponse kinetics, and light adaptation properties. Being on the other side of the spectrum from a typical cell that contains multiple G-protein types, rods and cones rely on conserved cell-specific G-protein heterotrimers: $G\alpha_{t1}/G\beta_1\gamma_1$ and $G\alpha_{t2}/G\beta_3\gamma_c$, respectively [31]. While trace expression levels of $G\gamma_2$ and $G\gamma_3$ subunits were detected in rods, their physiological contribution in phototransduction is negligible [32]. This property makes rods a unique model system to study the physiological roles of G-protein subunits in visual transduction by substituting individual rod-specific G-protein subunits with their cone-specific or ubiquitous isoforms. This experimental design was successful to show that when $G\alpha_{t1}$ was replaced by $G\alpha_{t2}$ in rods, while retaining native rod $G\beta_1\gamma_1$ complex, the phototransduction was largely unaffected [5–7].

To determine the physiological role of Gβγ in photoreceptor function, we previously genetically removed the gene *Gngt1* encoding rod $G\gamma_1$ subunit and demonstrated that the high light sensitivity of rods and their robust signal amplification are severely compromised in mice [2]. The $Gngt1^{-/-}$ model provided an excellent starting point to pose the next question of the possible physiological difference between various Gγ isoforms. Specifically, what is the reason for the selective use of $G\gamma_1$ and $G\gamma_c$ in rods and cones, respectively, and the exclusion of otherwise ubiquitously expressed $G\gamma_{11}$ from both photoreceptor types? This question is especially intriguing considering the fact that these three Gγ proteins belong to the same Class I Gγ subunits that are post-translationally modified by the shorter isoprenoid lipid farnesyl, as opposed to class II-IV Gγ subunits that are geranylgeranylated [33]. Farnesylation is required for proper targeting of G-proteins to the outer segment and full biological activity [34, 35]. Thus, replacing native rod $G\gamma_1$ with cone $G\gamma_c$ or $G\gamma_{11}$ subunit ensures highly controlled experimental conditions not affected by the Gγ class or isoprenylation differences.

Here, we generated three individual transgenic mouse lines expressing $G\gamma_c$, $G\gamma_{11}$, and control $G\gamma_1$ on the $Gngt1^{-/-}$ background (Fig 2). Immunohistochemical staining of retina cross-sections for the FLAG epitope that was included in all transgenic constructs showed similarly healthy retina morphology, uniform expression of these Gγ proteins and their proper targeting to the rod outer segments (Fig 3). The levels of expression of other major phototransduction proteins, such as rhodopsin, transducin subunits, and PDE were identical between the experimental and control retinas (Fig 4). Transgenic re-introduction of $G\gamma_1$, $G\gamma_c$, or $G\gamma_{11}$ also completely restored the levels of endogenous $G\alpha_{t1}$ (Fig 4) that is known to be severely reduced by the deletion of native $G\gamma_1$ [2, 3]. This result is of particular importance because signal

amplification in mammalian rods is directly proportional to the level of expression of their $G\alpha_{t1}$ subunit [27]. Thus, morphological and protein expression data argue that rods from the $G\gamma_1$, $G\gamma_c$, and $G\gamma_{11}$ transgenic lines are indistinguishable in their structure and protein complement.

Because Gβγ complexes function natively as inseparable heterodimers, the deletion of $G\gamma_1$ in rods is expected to lead to accumulation of misfolded $G\beta_1$ protein. Slow progressive retinal degeneration in the $G\gamma_1$ deficient mice was proposed to be the result of proteostatic stress, or inability of the rod cell ubiquitin-proteasome system to degrade un-complexed $G\beta_1$ protein effectively [36–39]. Expression of $G\gamma_1$, $G\gamma_c$, and $G\gamma_{11}$ in the $G\gamma_1$ deficient mice appears to rescue the retina degeneration phenotype independent of the type of the Gγ subunit, which argues for the productive complex formation of $G\beta_1\gamma_1$, $G\beta_1\gamma_c$, and $G\beta_1\gamma_{11}$ dimers and confirms previous biochemical results [40]. In addition, equal levels of the $G\alpha_{t1}$ expression in transgenic retinas (Fig 4) and effective delivery of $G\alpha_{t1}$ to the rod outer segments under dark adapted conditions (Fig 8) are consistent with normal heterotrimer formation and its proper subcellular localization.

There is a growing body of evidence that Gβγ-complexes contribute to the complexity and diversity of GPCR-mediated signaling that is shaped by specificity and response kinetics of GPCR/G-protein interactions at the plasma membrane, via direct interactions with effector molecules, as well as by acting at distant sites such as intracellular organelles [40, 41]. Thus, we examined whether Class I $G\gamma_1$, $G\gamma_c$, and $G\gamma_{11}$ modified by posttranslational farnesylation (Fig 1) would restore scotopic visual function, and to what extent they would determine rod photosensitivity and response kinetics. This question is especially intriguing while comparing and contrasting rod $G\gamma_1$ and cone $G\gamma_c$, as retinal rods respond to light at significantly lower light levels compared to cones, and rod response kinetics are markedly slower [42]. The results from our *in vivo* ERG experiments and single-cell suction electrode recordings conclusively demonstrate that despite minor variations, all three Class I Gγ subunits can support essentially normal scotopic rod photoresponses (Figs 5–7). Thus, the differences in Gγ composition between rods and cones cannot explain their unique activation properties in dark-adapted conditions. This also implies that Gγ involvement in the activation properties of photoreceptors per se has unlikely contributed to the evolutionary selection of $G\gamma_1$ for rods, $G\gamma_c$ for cones, and $G\gamma_{11}$ for other tissues. The physiological features determining selective expression of $G\gamma_1$ and $G\gamma_c$ in rods and cones is still to be determined. Our results mirror a previous observation obtained by replacing rod $G\alpha_{t1}$ by cone $G\alpha_{t2}$ that these two $G\alpha_t$ isoforms are functionally interchangeable [5]. Knowing that neither $G\alpha_{t2}$ nor $G\gamma_c$ makes the rod cascade activation cone-like, it remains quite possible that unique properties of cone phototransduction are determined by the $G\gamma_c$ counterpart $G\beta_3$ as part of the unique cone $G\beta_3\gamma_c$ complex, as deletion of $G\beta_3$ alone in cones doesn't affect cone response kinetics [43]. Alternatively, differences in upstream and downstream phototransduction components [44–46], as well as structural differences between rods and cones could account for their unique functional characteristics.

In stark contrast to the functional interchangeability of $G\gamma_1$, $G\gamma_c$, and $G\gamma_{11}$ in dark-adapted rod phototransduction, we observed a significant effect by the Gγ composition on the cell responsiveness in steady background light. Upon increasing the intensity of background illumination rod responses saturate quickly, the process accompanied by massive light-driven translocation of $G\alpha_{t1}$ from the rod outer to the rod inner segment [27]. While $G\alpha_{t1}$ translocation was similar in $G\gamma_1$ and $G\gamma_c$ transgenic retinas, substitution of $G\gamma_1$ with $G\gamma_{11}$ shifted the light threshold that triggers translocation to lower background light intensity by 2–3 orders of magnitude (Fig 8). We observed that transducin in $G\gamma_{11}$ transgenic rods began to translocate at a light intensity of just 1 Lux, while $G\gamma_1$ and $G\gamma_c$ transgenic rods were still deeply dark-adapted. This remarkable effect had profound implications on rod function, as only $G\gamma_{11}$

transgenic rods recovered their response amplitudes under a moderate steady background light, as observed in our transretinal ERG recordings (Fig 9).

While $G\gamma_{11}$ is normally excluded from rods and cones [15], and thus transducin heterotrimer $G\alpha_{t1}G\beta_1\gamma_{11}$ is likely not physiologically relevant, our results clearly demonstrate that in principle, the type of Gγ isoform can have significant implications for light adaptation and the kinetics of photoreceptors' escape from physiological saturation. Because $G\gamma_1$, $G\gamma_c$, and $G\gamma_{11}$ belong to the same class of farnesylated Gγ subunits, the observed effect must be attributed to the unique amino acid sequence of $G\gamma_{11}$ (Fig 1). Interestingly, a previous study utilizing the knock-in of the geranylgeranylated mutant of $G\gamma_1$ demonstrated normal photoresponses but impaired photoresponse recovery caused by the stronger interaction of the mutant protein with lipid membranes and compromised light-driven translocation of Gt [47], a predictably opposite effect to what we observed with $G\gamma_{11}$. Similarly, a recent study with mutant $G\alpha_{t1}$ that associates more strongly with $G\beta_1\gamma_1$ and as a result does not translocate efficiently in comparable background light, showed a suppressed recovery of the rod dark current under those conditions [30]. In the context of these findings, our results suggest that $G\alpha_{t1}$ associates more weekly with $G\beta_1\gamma_{11}$ than with the endogenous $G\beta_1\gamma_1$, causing easier dissociation and translocation upon light exposure. This conclusion is also supported by the comprehensive biochemical analysis of the heterotrimeric G-protein complex formation that demonstrated significantly weaker association of $G\beta_1\gamma_{11}$ compared to $G\beta_1\gamma_1$ with $G\alpha_{i1}$, a close relative of $G\alpha_{t1}$ [48]. Taken together, it appears that the Gγ-subunit amino acid sequence and the prenylation identity contribute to the unique physiological properties of rod photoreceptors under continuous illumination.

## Conclusion

By replacing the native $G\gamma_1$ subunit in mouse rod photoreceptors with cone-specific $G\gamma_c$ or ubiquitous $G\gamma_{11}$ isoforms, we examined the contribution of Gγ to the unique physiological properties of rods. Our results unequivocally show that while Class I Gγ subunits are functionally interchangeable in rod phototransduction, they control the light threshold for transducin translocation and the physiological light adaptation properties of rods.

## Supporting information

**S1 Raw images. Annotated Western blot images.**
(TIF)

## Acknowledgments

We thank Michael Casey and Elena Lomonosova for assistance in generating transgenic mice and Liesl Chi for assistance with the ERG experiments.

## Author Contributions

**Conceptualization:** Vladimir J. Kefalov, Oleg G. Kisselev.

**Data curation:** Alexander V. Kolesnikov, Elena Lobysheva, Vladimir J. Kefalov, Oleg G. Kisselev.

**Formal analysis:** Alexander V. Kolesnikov, Elena Lobysheva, Vladimir J. Kefalov, Oleg G. Kisselev.

**Funding acquisition:** Vladimir J. Kefalov, Oleg G. Kisselev.

**Investigation:** Alexander V. Kolesnikov, Elena Lobysheva, Vladimir J. Kefalov, Oleg G. Kisselev.

**Methodology:** Alexander V. Kolesnikov, Elena Lobysheva, Jaya P. Gnana-Prakasam, Vladimir J. Kefalov, Oleg G. Kisselev.

**Project administration:** Vladimir J. Kefalov, Oleg G. Kisselev.

**Resources:** Alexander V. Kolesnikov, Elena Lobysheva, Jaya P. Gnana-Prakasam, Vladimir J. Kefalov, Oleg G. Kisselev.

**Software:** Alexander V. Kolesnikov, Elena Lobysheva, Vladimir J. Kefalov, Oleg G. Kisselev.

**Supervision:** Vladimir J. Kefalov, Oleg G. Kisselev.

**Validation:** Alexander V. Kolesnikov, Elena Lobysheva, Vladimir J. Kefalov, Oleg G. Kisselev.

**Visualization:** Alexander V. Kolesnikov, Elena Lobysheva, Vladimir J. Kefalov, Oleg G. Kisselev.

**Writing – original draft:** Alexander V. Kolesnikov, Vladimir J. Kefalov, Oleg G. Kisselev.

**Writing – review & editing:** Alexander V. Kolesnikov, Jaya P. Gnana-Prakasam, Vladimir J. Kefalov, Oleg G. Kisselev.

## References

1. Arshavsky VY, Burns ME. Current understanding of signal amplification in phototransduction. Cellular logistics. 2014; 4:e29390. https://doi.org/10.4161/cl.29390 PMID: 25279249; PubMed Central PMCID: PMC4160332.
2. Kolesnikov AV, Rikimaru L, Hennig AK, Lukasiewicz PD, Fliesler SJ, Govardovskii VI, et al. G-protein betagamma-complex is crucial for efficient signal amplification in vision. J Neurosci. 2011; 31 (22):8067–77. Epub 2011/06/03. 31/22/8067 [pii] https://doi.org/10.1523/JNEUROSCI.0174-11.2011 PMID: 21632928; PubMed Central PMCID: PMC3118088.
3. Lobanova ES, Finkelstein S, Herrmann R, Chen YM, Kessler C, Michaud NA, et al. Transducin gamma-subunit sets expression levels of alpha- and beta-subunits and is crucial for rod viability. J Neurosci. 2008; 28(13):3510–20. https://doi.org/10.1523/JNEUROSCI.0338-08.2008 PMID: 18367617; PubMed Central PMCID: PMC2795350.
4. Chen CK, Woodruff ML, Chen FS, Shim H, Cilluffo MC, Fain GL. Replacing the rod with the cone transducin subunit decreases sensitivity and accelerates response decay. J Physiol. 2010; 588(Pt 17):3231–41. Epub 2010/07/07. https://doi.org/10.1113/jphysiol.2010.191221 jphysiol.2010.191221 [pii]. PMID: 20603337; PubMed Central PMCID: PMC2976018.
5. Deng WT, Sakurai K, Liu J, Dinculescu A, Li J, Pang J, et al. Functional interchangeability of rod and cone transducin alpha-subunits. Proc Natl Acad Sci U S A. 2009; 106(42):17681–6. Epub 2009/10/10. https://doi.org/10.1073/pnas.0901382106 0901382106 [pii]. PMID: 19815523; PubMed Central PMCID: PMC2758286.
6. Gopalakrishna KN, Boyd KK, Artemyev NO. Comparative analysis of cone and rod transducins using chimeric Galpha subunits. Biochemistry. 2012; 51(8):1617–24. Epub 2012/02/14. https://doi.org/10.1021/bi3000935 PMID: 22324825; PubMed Central PMCID: PMC3291952.
7. Mao W, Miyagishima KJ, Yao Y, Soreghan B, Sampath AP, Chen J. Functional comparison of rod and cone Galpha(t) on the regulation of light sensitivity. Journal of Biological Chemistry. 2013; 288(8):5257–67. Epub 2013/01/05. https://doi.org/10.1074/jbc.M112.430058 M112.430058 [pii]. PMID: 23288843; PubMed Central PMCID: PMC3581426.
8. Gautam N, Downes GB, Yan K, Kisselev O. The G-protein betagamma complex. Cell Signal. 1998; 10 (7):447–55. https://doi.org/10.1016/s0898-6568(98)00006-0 PMID: 9754712.
9. Downes GB, Gautam N. The G protein subunit gene families. Genomics. 1999; 62(3):544–52. https://doi.org/10.1006/geno.1999.5992 PMID: 10644457.
10. Smrcka AV. G protein betagamma subunits: central mediators of G protein-coupled receptor signaling. Cell Mol Life Sci. 2008; 65(14):2191–214. Epub 2008/05/20. https://doi.org/10.1007/s00018-008-8006-5 PMID: 18488142; PubMed Central PMCID: PMC2688713.

11. McIntire WE. Structural determinants involved in the formation and activation of G protein betagamma dimers. Neurosignals. 2009; 17(1):82–99. Epub 2009/02/13. 000186692 [pii] https://doi.org/10.1159/000186692 PMID: 19212142; PubMed Central PMCID: PMC2836951.

12. Hurley JB, Fong HK, Teplow DB, Dreyer WJ, Simon MI. Isolation and characterization of a cDNA clone for the gamma subunit of bovine retinal transducin. Proc Natl Acad Sci U S A. 1984; 81(22):6948–52. https://doi.org/10.1073/pnas.81.22.6948 PMID: 6438626.

13. Ong OC, Yamane HK, Phan KB, Fong HK, Bok D, Lee RH, et al. Molecular cloning and characterization of the G protein gamma subunit of cone photoreceptors. Journal of Biological Chemistry. 1995; 270 (15):8495–500. https://doi.org/10.1074/jbc.270.15.8495 PMID: 7721746

14. Morishita R, Ueda H, Kato K, Asano T. Identification of two forms of the gamma subunit of G protein, gamma10 and gamma11, in bovine lung and their tissue distribution in the rat [In Process Citation]. FEBS Lett. 1998; 428:85–8. https://doi.org/10.1016/s0014-5793(98)00498-0 PMID: 9645481

15. Balcueva EA, Wang Q, Hughes H, Kunsch C, Yu Z, Robishaw JD. Human G protein gamma(11) and gamma(14) subtypes define a new functional subclass. Experimental cell research. 2000; 257(2):310–9. https://doi.org/10.1006/excr.2000.4893 PMID: 10837145.

16. Cali JJ, Balcueva EA, Rybalkin I, Robishaw JD. Selective tissue distribution of G protein gamma subunits, including a new form of the gamma subunits identified by cDNA cloning. The Journal of biological chemistry. 1992; 267(33):24023–7. PMID: 1385432.

17. Krumins AM, Gilman AG. Targeted knockdown of G protein subunits selectively prevents receptor-mediated modulation of effectors and reveals complex changes in non-targeted signaling proteins. Journal of Biological Chemistry. 2006; 281(15):10250–62. Epub 2006/02/01. M511551200 [pii] https://doi.org/10.1074/jbc.M511551200 PMID: 16446365.

18. Kisselev OG, Kolesnikov AV, Lobysheva EL, Kefalov VJ. Replacement of rod-specific transducin gamma subunit in mouse rod photoreceptors. FASEB, Biology and Chemistry of Vision, Steamboat Springs, CO, June 9 –June 14,. 2013.

19. Lem J, Applebury ML, Falk JD, Flannery JG, Simon MI. Tissue-specific and developmental regulation of rod opsin chimeric genes in transgenic mice. Neuron. 1991; 6(2):201–10. Epub 1991/02/01. 0896-6273(91)90356-5 [pii]. https://doi.org/10.1016/0896-6273(91)90356-5 PMID: 1825171.

20. Cheng CL, Djajadi H, Molday RS. Cell-specific markers for the identification of retinal cells by immunofluorescence microscopy. Methods in molecular biology. 2013; 935:185–99. https://doi.org/10.1007/978-1-62703-080-9_12 PMID: 23150368.

21. Kolesnikov AV, Maeda A, Tang PH, Imanishi Y, Palczewski K, Kefalov VJ. Retinol dehydrogenase 8 and ATP-binding cassette transporter 4 modulate dark adaptation of M-cones in mammalian retina. J Physiol. 2015; 593(22):4923–41. https://doi.org/10.1113/JP271285 PMID: 26350353; PubMed Central PMCID: PMC4650407.

22. Pugh EN Jr., Lamb TD. Amplification and kinetics of the activation steps in phototransduction. Biochim Biophys Acta. 1993; 1141(2–3):111–49. Epub 1993/03/01. https://doi.org/10.1016/0005-2728(93)90038-h PMID: 8382952.

23. Pepperberg DR, Cornwall MC, Kahlert M, Hofmann KP, Jin J, Jones GJ, et al. Light-dependent delay in the falling phase of the retinal rod photoresponse. Vis Neurosci. 1992; 8(1):9–18. Epub 1992/01/01. https://doi.org/10.1017/s0952523800006441 PMID: 1739680.

24. Vinberg F, Kolesnikov AV, Kefalov VJ. Ex vivo ERG analysis of photoreceptors using an in vivo ERG system. Vision Res. 2014; 101:108–17. Epub 20140621. https://doi.org/10.1016/j.visres.2014.06.003 PMID: 24959652; PubMed Central PMCID: PMC4149224.

25. Sillman AJ, Ito H, Tomita T. Studies on the mass receptor potential of the isolated frog retina. I. General properties of the response. Vision research. 1969; 9(12):1435–42. Epub 1969/12/01. 0042-6989(69)90059-5 [pii]. https://doi.org/10.1016/0042-6989(69)90059-5 PMID: 5367433.

26. Nymark S, Heikkinen H, Haldin C, Donner K, Koskelainen A. Light responses and light adaptation in rat retinal rods at different temperatures. J Physiol. 2005; 567(Pt 3):923–38. Epub 20050721. https://doi.org/10.1113/jphysiol.2005.090662 PMID: 16037091; PubMed Central PMCID: PMC1474229.

27. Sokolov M, Lyubarsky AL, Strissel KJ, Savchenko AB, Govardovskii VI, Pugh EN, Jr., et al. Massive light-driven translocation of transducin between the two major compartments of rod cells: a novel mechanism of light adaptation. Neuron. 2002; 34(1):95–106. Epub 2002/04/05. S0896627302006360 [pii]. https://doi.org/10.1016/s0896-6273(02)00636-0 PMID: 11931744.

28. Potter C, Zhu W, Razafsky D, Ruzycki P, Kolesnikov AV, Doggett T, et al. Multiple Isoforms of Nesprin1 Are Integral Components of Ciliary Rootlets. Current biology: CB. 2017; 27(13):2014–22 e6. https://doi.org/10.1016/j.cub.2017.05.066 PMID: 28625779; PubMed Central PMCID: PMC5546243.

29. Lobanova ES, Finkelstein S, Song H, Tsang SH, Chen CK, Sokolov M, et al. Transducin translocation in rods is triggered by saturation of the GTPase-activating complex. J Neurosci. 2007; 27(5):1151–60.

https://doi.org/10.1523/JNEUROSCI.5010-06.2007 PMID: 17267570; PubMed Central PMCID: PMC6673185.

30. Frederiksen R, Morshedian A, Tripathy SA, Xu T, Travis GH, Fain GL, et al. Rod Photoreceptors Avoid Saturation in Bright Light by the Movement of the G Protein Transducin. J Neurosci. 2021; 41 (15):3320–30. https://doi.org/10.1523/JNEUROSCI.2817-20.2021 PMID: 33593858; PubMed Central PMCID: PMC8051685.

31. Peng YW, Robishaw JD, Levine MA, Yau KW. Retinal rods and cones have distinct G protein beta and gamma subunits. Proc Natl Acad Sci U S A. 1992; 89(22):10882–6. https://doi.org/10.1073/pnas.89.22.10882 PMID: 1438293; PubMed Central PMCID: PMC50446.

32. Dexter PM, Lobanova ES, Finkelstein S, Spencer WJ, Skiba NP, Arshavsky VY. Transducin beta-Subunit Can Interact with Multiple G-Protein gamma-Subunits to Enable Light Detection by Rod Photoreceptors. eNeuro. 2018; 5(3). https://doi.org/10.1523/ENEURO.0144-18.2018 PMID: 29911170; PubMed Central PMCID: PMC6001135.

33. Chen H, Leung T, Giger KE, Stauffer AM, Humbert JE, Sinha S, et al. Expression of the G protein gammaT1 subunit during zebrafish development. Gene expression patterns: GEP. 2007; 7(5):574–83. https://doi.org/10.1016/j.modgep.2007.01.003 PMID: 17306630; PubMed Central PMCID: PMC2754307.

34. Brooks C, Murphy J, Belcastro M, Heller D, Kolandaivelu S, Kisselev O, et al. Farnesylation of the Transducin G Protein Gamma Subunit Is a Prerequisite for Its Ciliary Targeting in Rod Photoreceptors. Frontiers in molecular neuroscience. 2018; 11:16. https://doi.org/10.3389/fnmol.2018.00016 PMID: 29410614; PubMed Central PMCID: PMC5787109.

35. Matsuda T, Hashimoto Y, Ueda H, Asano T, Matsuura Y, Doi T, et al. Specific isoprenyl group linked to transducin gamma-subunit is a determinant of its unique signaling properties among G-proteins. Biochemistry. 1998; 37(27):9843–50. https://doi.org/10.1021/bi973194c PMID: 9657698.

36. Brooks C, Snoberger A, Belcastro M, Murphy J, Kisselev OG, Smith DM, et al. Archaeal Unfoldase Counteracts Protein Misfolding Retinopathy in Mice. J Neurosci. 2018; 38(33):7248–54. https://doi.org/10.1523/JNEUROSCI.0905-18.2018 PMID: 30012684; PubMed Central PMCID: PMC6096037.

37. Dexter PM, Lobanova ES, Finkelstein S, Arshavsky VY. Probing Proteostatic Stress in Degenerating Photoreceptors Using Two Complementary In Vivo Reporters of Proteasomal Activity. eNeuro. 2020; 7 (1). https://doi.org/10.1523/ENEURO.0428-19.2019 PMID: 31826915; PubMed Central PMCID: PMC6948925.

38. Lobanova ES, Finkelstein S, Li J, Travis AM, Hao Y, Klingeborn M, et al. Increased proteasomal activity supports photoreceptor survival in inherited retinal degeneration. Nature communications. 2018; 9 (1):1738. https://doi.org/10.1038/s41467-018-04117-8 PMID: 29712894; PubMed Central PMCID: PMC5928105.

39. Lobanova ES, Finkelstein S, Skiba NP, Arshavsky VY. Proteasome overload is a common stress factor in multiple forms of inherited retinal degeneration. Proc Natl Acad Sci U S A. 2013; 110(24):9986–91. https://doi.org/10.1073/pnas.1305521110 PMID: 23716657; PubMed Central PMCID: PMC3683722.

40. Masuho I, Skamangas NK, Muntean BS, Martemyanov KA. Diversity of the Gbetagamma complexes defines spatial and temporal bias of GPCR signaling. Cell systems. 2021; 12(4):324–37 e5. https://doi.org/10.1016/j.cels.2021.02.001 PMID: 33667409; PubMed Central PMCID: PMC8068604.

41. Tennakoon M, Senarath K, Kankanamge D, Ratnayake K, Wijayaratna D, Olupothage K, et al. Subtype-dependent regulation of Gbetagamma signalling. Cell Signal. 2021; 82:109947. Epub 20210211. https://doi.org/10.1016/j.cellsig.2021.109947 PMID: 33582184; PubMed Central PMCID: PMC8026654.

42. Kolesnikov AV, Kisselev OG, Kefalov VJ. Signaling by rod and cone photoreceptors: opsin properties, G-protein assembly, and mechanisms of activation. Martemyanov K A, Sampath A P (Eds), G Protein Signaling Mechanisms in the Retina, Springer. 2014:23–48.

43. Nikonov SS, Lyubarsky A, Fina ME, Nikonova ES, Sengupta A, Chinniah C, et al. Cones respond to light in the absence of transducin beta subunit. J Neurosci. 2013; 33(12):5182–94. https://doi.org/10.1523/JNEUROSCI.5204-12.2013 PMID: 23516284; PubMed Central PMCID: PMC3866503.

44. Kawamura S, Tachibanaki S. Rod and cone photoreceptors: molecular basis of the difference in their physiology. Comparative biochemistry and physiology Part A, Molecular & integrative physiology. 2008; 150(4):369–77. https://doi.org/10.1016/j.cbpa.2008.04.600 PMID: 18514002.

45. Kefalov V, Fu Y, Marsh-Armstrong N, Yau KW. Role of visual pigment properties in rod and cone phototransduction. Nature. 2003; 425(6957):526–31. https://doi.org/10.1038/nature01992 PMID: 14523449; PubMed Central PMCID: PMC2581816.

46. Kefalov VJ, Estevez ME, Kono M, Goletz PW, Crouch RK, Cornwall MC, et al. Breaking the covalent bond—a pigment property that contributes to desensitization in cones. Neuron. 2005; 46(6):879–90.

https://doi.org/10.1016/j.neuron.2005.05.009 PMID: 15953417; PubMed Central PMCID: PMC2885911.

47. Kassai H, Aiba A, Nakao K, Nakamura K, Katsuki M, Xiong WH, et al. Farnesylation of retinal transducin underlies its translocation during light adaptation. Neuron. 2005; 47(4):529–39. https://doi.org/10.1016/j.neuron.2005.07.025 PMID: 16102536; PubMed Central PMCID: PMC2885908.

48. Hillenbrand M, Schori C, Schoppe J, Pluckthun A. Comprehensive analysis of heterotrimeric G-protein complex diversity and their interactions with GPCRs in solution. Proc Natl Acad Sci U S A. 2015; 112 (11):E1181–90. Epub 20150302. https://doi.org/10.1073/pnas.1417573112 PMID: 25733868; PubMed Central PMCID: PMC4371982.